AIAA JOURNAL
Vol. 35, No. 8, August 1997

Extending Sensitivity-Based Updating to Lightly Damped Structures

Gregory W. Brown* and Charbel Farhat†
University of Colorado, Boulder, Colorado 80309-0429
and
François M. Hemez‡
École Centrale Paris, Châtenay-Malabry 92295, France

The sensitivity-based element-by-element (SB-EBE) method is extended for updating the finite element models of lightly damped structures using experimentally measured complex modes. The new updating method proceeds in two steps. First, the measured mode shapes are expanded and the mass and stiffness matrices are corrected to minimize a set of dynamic residuals. Next, a damping matrix is constructed to absorb the remainder of these dynamic residuals. As the mass and stiffness matrices are corrected before the computation of the damping matrix, the extension is used for the updating of lightly damped structures. The new SB-EBE method is illustrated with two examples that highlight its potential for refining the finite element models of lightly damped structures.

I. Introduction

ACCURATE models of space structures are required for the prediction of on-orbit dynamics and the adjustment of control laws. Therefore, the correlation of finite element (FE) models with experimental data is used to correct potential modeling errors. The update of FE models can also be used as a damage detection scheme[1] and, therefore, as a nondestructive evaluation method of the integrity of a structure. The sensitivity-based element-by-element (SB-EBE)[2,3] method is one among several procedures for updating FE models. These approaches include Lagrange multiplier methods,[4–6] matrix adjustment or matrix perturbation,[7–9] statistics and sensitivity methods,[10–13] force balance methods,[14,15] updating using frequency response data,[16,17] and substructure by substructure or element-by-element procedures.[18,19] Reviews of FE model updating methods have been written by Ibrahim and Saafin,[20] Caesar,[21] and Heylen and Sas.[22] For dynamic prediction, an estimation of system damping is often required. One approach is to build a model of the system damping by detailed modeling of different damping effects.[23] However, this may not be practical due to the complexity and variety of different materials found in larger structures. In addition, any such model will still need to be verified against experimental measurement of the assembled structure. Often, a damping matrix is constructed from modal test data. In practice, the off-diagonal terms of the modal damping matrix are often neglected, possibly leading to errors.[24] The modal damping matrix is often transformed into the space of the FE coordinates. However, this transformation can lead to a full matrix, which may cause problems for large-scale FE models that usually require the use of sparse storage schemes.

To alleviate some of these difficulties when dealing with lightly damped structures, an extension to the original SB-EBE method using complex modes shapes is proposed. Previous work with complex modes often led to predictive models that destroyed the physical meaning of the system or forced restriction of the model to the measured degrees of freedom.[25] By extending SB-EBE, the damping matrix is corrected through changes in design parameters, rather than by changing entries in the damping matrix. This maintains the connectivity of the FE matrices and provides a physical basis for the update.

The extension discussed herein is a two-step procedure for the updating of lightly damped systems. First, the mass and stiffness matrices are corrected using a variant of the original SB-EBE method. Then, the damping matrix is computed using the corrected mass and stiffness matrices and the expanded complex mode shapes. For linear models of damping, no iteration is required in the correction of the damping matrix. Therefore, the method is almost computationally equivalent to correcting only the mass and stiffness matrices using the original SB-EBE procedure.

A review of the original SB-EBE method is first given. Next, the extension is explained, highlighting its main features. Two test problems are presented to validate the method. A simple 10-degree-of-freedom problem is used to illustrate the effect of the amount of damping on the update of the mass and stiffness matrices and the computation of the damping matrix. A large test problem simulating a real truss structure is presented and discussed.

II. SB-EBE Method

We discuss an extension to the SB-EBE procedure for the updating of lightly damped structures. Therefore, a brief overview of the original SB-EBE method is presented to keep this paper self-contained.

Correction of the mass and stiffness matrices is done at the element level through the adjustment of design parameters, such as area, elastic modulus, and density. Minimization of the modal residuals[14] representing out-of-balance forces forms the basis of this formulation. The superscripts A, E, and U are used to identify analytic (FE), experimental (measured), and updated quantities, respectively. The subscripts M and NM denote measured and unmeasured degrees of freedom, respectively, in a matrix or vector. The analytic mass matrix $\boldsymbol{M}$ and analytic stiffness matrix $\boldsymbol{K}$ satisfy the undamped free-vibration equations of motion

$$\boldsymbol{K}^A\boldsymbol{\Phi}_i^A - \Omega_i^{A2}\boldsymbol{M}^A\boldsymbol{\Phi}_i^A = 0 \qquad \text{for} \qquad i = 1, \ldots, m \tag{1}$$

where m is the number of normal modes; Ω^2 and $\boldsymbol{\Phi}$ are the set of normal (undamped) eigenvalues and set of normal mode shapes, respectively. However, the free-vibration equations are generally not satisfied for the FE matrices and experimental data, so that

$$\boldsymbol{K}^A\boldsymbol{\Phi}_i^E - \Omega_i^{E2}\boldsymbol{M}^A\boldsymbol{\Phi}_i^E \neq 0 \qquad \text{for} \qquad i = 1, \ldots, m \tag{2}$$

Equation (2) assumes that the FE model and experimental model are of the same size. However, in most cases, the experimental data have fewer degrees of freedom than the FE model. To overcome this deficiency, two approaches are commonly used. One possibility is

Received Dec. 11, 1996; revision received April 21, 1997; accepted for publication April 24, 1997.

*Research Assistant, Department of Aerospace Engineering Sciences and Center for Space Construction. Member AIAA.

†Professor, Department of Aerospace Engineering Sciences and Center for Space Construction. Associate Fellow AIAA.

‡Assistant Professor, Department of Mechanical Engineering of Soils, Structures, and Materials and French National Center for Scientific Research (Unité Recherche Associée 850). Member AIAA.

to condense the FE model to the measured degrees of freedom.[26] However, this destroys the connectivity of the original model, thus preventing a straightforward physical understanding of the update. Instead, SB-EBE utilizes a modal expansion technique whereby the experimental modes are expanded to the same number of degrees of freedom as the FE model. This can be written as

$$\boldsymbol{\Phi}_i^E = \begin{bmatrix} \boldsymbol{\Phi}_{iM}^E \\ \boldsymbol{\Phi}_{iNM}^E \end{bmatrix} \qquad \text{for} \qquad i = 1, \ldots, m \tag{3}$$

The objective of the update is to determine the updated matrices $\boldsymbol{K}^U = \boldsymbol{K}^A + \Delta\boldsymbol{K}$ and $\boldsymbol{M}^U = \boldsymbol{M}^A + \Delta\boldsymbol{M}$ to satisfy

$$\boldsymbol{K}^U \begin{bmatrix} \boldsymbol{\Phi}_{iM}^E \\ \boldsymbol{\Phi}_{iNM}^E \end{bmatrix} - \Omega_i^{E2} \boldsymbol{M}^U \begin{bmatrix} \boldsymbol{\Phi}_{iM}^E \\ \boldsymbol{\Phi}_{iNM}^E \end{bmatrix} = 0 \qquad \text{for} \qquad i = 1, \ldots, m \tag{4}$$

Thus, the unknowns in the updating process are the adjustments to the FE matrices $\Delta\boldsymbol{K}$ and $\Delta\boldsymbol{M}$, as well as the modal expansions $\boldsymbol{\Phi}_{NM}^E$. The updating problem is formulated as the minimization of the following functional for each mode:

$$H_i = \left\| (\boldsymbol{K}^A + \Delta\boldsymbol{K}) \begin{bmatrix} \boldsymbol{\Phi}_{iM}^E \\ \boldsymbol{\Phi}_{iNM}^E \end{bmatrix} - \Omega_i^{E2} (\boldsymbol{M}^A + \Delta\boldsymbol{M}) \begin{bmatrix} \boldsymbol{\Phi}_{iM}^E \\ \boldsymbol{\Phi}_{iNM}^E \end{bmatrix} \right\|_2 \qquad \text{for} \qquad i = 1, \ldots, m \tag{5}$$

This minimization corresponds physically to the reduction of the modal residuals, representing out-of-balance forces. Because this is a nonlinear optimization problem, a staggered algorithm is used. At each iteration n, the expanded mode shapes $\boldsymbol{\Phi}_{NM}^E$ are computed based on the mass and stiffness matrices at the previous iteration. The mode expansions at iteration n are found by taking the first variation of the functionals, H. Note that the adjustments to the FE matrices are fixed at the value of the preceding iteration, $(n-1)$. The expansions are found by the solution to the equations

$$\frac{\partial H_i(\Delta\boldsymbol{K}^{(n-1)}, \Delta\boldsymbol{M}^{(n-1)})}{\partial \boldsymbol{\Phi}_{iNM}} = 0 \qquad \text{for} \qquad i = 1, \ldots, m \tag{6}$$

Following the mode expansion step, the update matrices at iteration n are determined based on the mode expansions $\boldsymbol{\Phi}_{NM}^{E(n)}$ and the update matrices at the previous iteration, $\Delta\boldsymbol{K}^{(n-1)}$ and $\Delta\boldsymbol{M}^{(n-1)}$. The update matrices are approximated by the first-order Taylor series expansions with respect to the set of model design parameters $\boldsymbol{p}$:

$$\Delta\boldsymbol{K} = \boldsymbol{K}(\boldsymbol{p} + \delta\boldsymbol{p}) - \boldsymbol{K}(\boldsymbol{p}) \approx \left[\frac{\partial \boldsymbol{K}(\boldsymbol{p})}{\partial \boldsymbol{p}} \right] \delta\boldsymbol{p} \tag{7}$$

$$\Delta\boldsymbol{M} = \boldsymbol{M}(\boldsymbol{p} + \delta\boldsymbol{p}) - \boldsymbol{M}(\boldsymbol{p}) \approx \left[\frac{\partial \boldsymbol{M}(\boldsymbol{p})}{\partial \boldsymbol{p}} \right] \delta\boldsymbol{p} \tag{8}$$

where $\delta\boldsymbol{p}$ are the adjustments to the set of model design parameters. Using the assembly property of FEs, the preceding update matrices can be rewritten in terms of the element stiffness matrix $\boldsymbol{k}$ and element mass matrix $\boldsymbol{m}$:

$$\Delta\boldsymbol{K} \approx \sum_{e=1}^{N_e} \sum_{k=1}^{N_p^{(e)}} \left[\frac{\partial \boldsymbol{k}_e(\boldsymbol{p})}{\partial p_k} \right] \delta p_k \tag{9}$$

$$\Delta\boldsymbol{M} \approx \sum_{e=1}^{N_e} \sum_{k=1}^{N_p^{(e)}} \left[\frac{\partial \boldsymbol{m}_e(\boldsymbol{p})}{\partial p_k} \right] \delta p_k \tag{10}$$

where N_e is the total number of FEs in the mesh and $N_p^{(e)}$ is the number of design parameters for FE number e. Note that, in principle, only small perturbations $\delta\boldsymbol{p}$ should be considered due to the Taylor series expansions. However, in practice, the element level matrices are often linear functions of the design parameters. Thus, arbitrary large adjustments become acceptable. With the preceding expressions, the unknowns of the FE matrices correction step become the adjustments to the design parameters, $\delta\boldsymbol{p}$. The first variation of the functionals, H, is taken to give a system of equations to solve for the design parameter adjustments. This is written as

$$\frac{\partial H_i(\boldsymbol{\Phi}_{iNM}^{E(n)}, \Delta\boldsymbol{K}^{(n-1)}, \Delta\boldsymbol{M}^{(n-1)})}{\partial \delta\boldsymbol{p}} = 0 \qquad \text{for} \qquad i = 1, \ldots, m \tag{11}$$

This correction system is usually overdetermined. The parameter adjustments $\delta\boldsymbol{p}$ are determined using a singular value decomposition (SVD) factorization. The new design parameters $\boldsymbol{p}^{(n)} = \boldsymbol{p}^{(n-1)} + \delta\boldsymbol{p}^{(n)}$ are then used to build the updated mass and stiffness matrices. At the next iteration, these new mass and stiffness matrices are used to determine the revised mode expansions. Because changes to the FE matrices are built at the element level through increments in the design parameters, the connectivity of the structure remains unchanged and physical meaning for the correction is provided.

In many cases, the errors of the FE model are concentrated in localized areas of the mesh. To obtain computational efficiency, SB-EBE uses a feature known as zooming. By examining the partial variations of the modal residuals with respect to the design parameters, the algorithm locates the dominating error locations. Thus, CPU time is not spent correcting error-free regions of the model, and spreading of the correction is avoided.

Frequently, numerical difficulties arise from the disproportion between the mass derived and stiffness derived equations of the correction system. To alleviate much of this difficulty, a modified SVD solver and a dimensionless procedure have been developed.[27] The scaling of physical quantities to obtain dimensionless units is equivalent to scaling each column of the correction system.

In general, SB-EBE provides a robust updating methodology for systems where damping information is not required and normal modes are available.

III. Algorithm for Updating of Lightly Damped Systems

A. Basis of Formulation

To deal with damped systems, an extension of SB-EBE is proposed. This is a two-step procedure using complex modes to update damped dynamical models. As in the original SB-EBE, the new method updates the model through changes in design parameters. Fundamentally, the proposed method attempts first to update the mass and stiffness matrices to match the experimental data as close as possible. Then it corrects the damping matrix to account for the remaining error. Because complex modes are used for updating of the mass and stiffness matrices prior to inclusion of the damping matrix, the extension is used for the updating of lightly damped systems. Owing to the two-step arrangement, iteration is usually not required to update the damping matrix. As in the original SB-EBE, the minimization of modal residuals is the basis of this formulation.

The superscripts real and imag are used to denote, respectively, the real and imaginary parts of a complex quantity. The FE mass matrix $\boldsymbol{M}$, stiffness matrix $\boldsymbol{K}$, and damping matrix $\boldsymbol{D}$ satisfy the complex eigenvalue problem

$$\lambda_i^{A2} \boldsymbol{M}^A \boldsymbol{\Psi}_i^A + \lambda_i^A \boldsymbol{D}^A \boldsymbol{\Psi}_i^A + \boldsymbol{K}^A \boldsymbol{\Psi}_i^A = 0 \quad \text{for} \quad i = 1, \ldots, c \tag{12}$$

where $\lambda_i = \sigma_i + j\omega_i$ and $\boldsymbol{\Psi}_i = \boldsymbol{\Psi}_i^{\text{real}} + j\boldsymbol{\Psi}_i^{\text{imag}}$ are, respectively, the complex eigenvalue and eigenvector of mode i, noting that $j = \sqrt{-1}$. Here, c is the number of complex modes. Equating real and imaginary terms yields two equations. Rearranging to group damping terms and making the leading coefficient of the mass matrix equal to the complex modulus gives the following equations:

$$\left\{ \left[-(\sigma_i^{A2} + \omega_i^{A2}) \boldsymbol{M}^A + \boldsymbol{K}^A \right] \boldsymbol{\Psi}_i^{\text{real}\,A} \right\} - \left\{ \left[2\sigma_i^{A2} \boldsymbol{M}^A + \sigma_i^A \boldsymbol{D}^A \right] \times \boldsymbol{\Psi}_i^{\text{real}\,A} - \left[2\sigma_i^A \omega_i^A \boldsymbol{M}^A + \omega_i^A \boldsymbol{D}^A \right] \boldsymbol{\Psi}_i^{\text{imag}\,A} \right\} = 0 \qquad \text{for} \qquad i = 1, \ldots, c \tag{13}$$

$$\left\{ \left[-(\sigma_i^{A2} + \omega_i^{A2}) \boldsymbol{M}^A + \boldsymbol{K}^A \right] \boldsymbol{\Psi}_i^{\text{imag}\,A} \right\} - \left\{ \left[2\sigma_i^{A2} \boldsymbol{M}^A + \sigma_i^A \boldsymbol{D}^A \right] \times \boldsymbol{\Psi}_i^{\text{imag}\,A} + \left[2\sigma_i^A \omega_i^A \boldsymbol{M}^A + \omega_i^A \boldsymbol{D}^A \right] \boldsymbol{\Psi}_i^{\text{real}\,A} \right\} = 0 \qquad \text{for} \qquad i = 1, \ldots, c \tag{14}$$

However, when the experimental complex modal data is used with the FE matrices, these equations are usually not satisfied. As with

the original SB-EBE procedure, modal expansion is used. The experimental mode shapes, therefore, are written as

$$\Psi_i^E = \begin{bmatrix} \Psi_{iM}^{\text{real } E} \\ \Psi_{iNM}^{\text{real } E} \end{bmatrix} + j \begin{bmatrix} \Psi_{iM}^{\text{imag } E} \\ \Psi_{iNM}^{\text{imag } E} \end{bmatrix} \qquad \text{for} \qquad i = 1, \ldots, c \quad (15)$$

The updated FE damping matrix is defined as

$$\boldsymbol{D}^U = \boldsymbol{D}^A + \Delta \boldsymbol{D} \quad (16)$$

We wish to find the mode expansions and updated matrices as defined earlier such that the following equations are satisfied:

$$\left\{ [-(\sigma_i^{E2} + \omega_i^{E2})\boldsymbol{M}^U + \boldsymbol{K}^U] \begin{bmatrix} \Psi_{iM}^{\text{real } E} \\ \Psi_{iNM}^{\text{real } E} \end{bmatrix} \right\} - \left\{ [2\sigma_i^{E2}\boldsymbol{M}^U + \sigma_i^E \boldsymbol{D}^U] \begin{bmatrix} \Psi_{iM}^{\text{real } E} \\ \Psi_{iNM}^{\text{real } E} \end{bmatrix} - [2\sigma_i^E \omega_i^E \boldsymbol{M}^U + \omega_i^E \boldsymbol{D}^U] \times \begin{bmatrix} \Psi_{iM}^{\text{imag } E} \\ \Psi_{iNM}^{\text{imag } E} \end{bmatrix} \right\} = 0 \qquad \text{for} \qquad i = 1, \ldots, c \quad (17)$$

$$\left\{ [-(\sigma_i^{E2} + \omega_i^{E2})\boldsymbol{M}^U + \boldsymbol{K}^U] \begin{bmatrix} \Psi_{iM}^{\text{imag } E} \\ \Psi_{iNM}^{\text{imag } E} \end{bmatrix} \right\} - \left\{ [2\sigma_i^{E2}\boldsymbol{M}^U + \sigma_i^E \boldsymbol{D}^U] \begin{bmatrix} \Psi_{iM}^{\text{imag } E} \\ \Psi_{iNM}^{\text{imag } E} \end{bmatrix} + [2\sigma_i^E \omega_i^E \boldsymbol{M}^U + \omega_i^E \boldsymbol{D}^U] \times \begin{bmatrix} \Psi_{iM}^{\text{real } E} \\ \Psi_{iNM}^{\text{real } E} \end{bmatrix} \right\} = 0 \qquad \text{for} \qquad i = 1, \ldots, c \quad (18)$$

The unknowns in the preceding sets of equations are the adjustments to the FE matrices, $\Delta \boldsymbol{K}$, $\Delta \boldsymbol{M}$, and $\Delta \boldsymbol{D}$. There are also the additional unknowns of the modal expansions Ψ_{NM}^E resulting from the deficient degrees of freedom of the experimental data. Thus, we have a coupled nonlinear optimization problem. We propose to solve this problem in two steps. First, the mass and stiffness matrices are corrected as if the system were undamped. This is done by forcing the first terms of Eqs. (17) and (18) to be as small as possible. This approach is a variant of the original SB-EBE, but note that the modulus of the complex eigenvalue now appears as the coefficient of the mass matrix. Then, in the second step, the updated mass and stiffness matrices, along with the expanded complex mode shapes, are used to correct the damping matrix. The two steps of this process are explained in further detail in the subsections to follow.

The damping matrix is corrected based on a user-defined model. Therefore, different damping models can be used within the confines of this method. The chosen model could be as simple as a two-parameter proportional damping model, or more complex, such as element level proportional damping or damping FEs based on detailed modeling of various damping effects. Working within the confines of the user-defined model provides insight into the damping mechanisms of the structure. In short, the method will attempt to reproduce the experimental data as well as possible using the model template provided. When using damping models that depend linearly on the design parameters, we will show that no initial damping matrix is required and no iteration is necessary for the computation of the damping matrix.

B. Expansion of Mode Shapes and Updating of Mass and Stiffness Matrices

The first step of the process expands the mode shapes and updates the mass and stiffness matrices with a variant of SB-EBE, using complex modes. The basis of this step is the minimization of the following functionals representing the first terms of Eqs. (17) and (18):

$$J_i = \left\| (\boldsymbol{K}^A + \Delta \boldsymbol{K}) \begin{bmatrix} \Psi_{iM}^{\text{real } E} \\ \Psi_{iNM}^{\text{real } E} \end{bmatrix} - (\boldsymbol{M}^A + \Delta \boldsymbol{M}) \begin{bmatrix} \Psi_{iM}^{\text{real } E} \\ \Psi_{iNM}^{\text{real } E} \end{bmatrix} \times (\sigma_i^{E2} + \omega_i^{E2}) \right\|_2 \qquad \text{for} \qquad i = 1, \ldots, c \quad (19)$$

$$K_i = \left\| (\boldsymbol{K}^A + \Delta \boldsymbol{K}) \begin{bmatrix} \Psi_{iM}^{\text{imag } E} \\ \Psi_{iNM}^{\text{imag } E} \end{bmatrix} - (\boldsymbol{M}^A + \Delta \boldsymbol{M}) \begin{bmatrix} \Psi_{iM}^{\text{imag } E} \\ \Psi_{iNM}^{\text{imag } E} \end{bmatrix} \times (\sigma_i^{E2} + \omega_i^{E2}) \right\|_2 \qquad \text{for} \qquad i = 1, \ldots, c \quad (20)$$

Note that a set of functionals arises from both the real and imaginary equations. The unknowns in this step of the process are the adjustments of the mass and stiffness matrices $\Delta \boldsymbol{M}$ and $\Delta \boldsymbol{K}$ and the unmeasured complex mode shape components Ψ_{NM}^E. As before, an iterative method will be used. At each iteration n, the expanded mode shapes $\Psi_{NM}^{E(n)}$ are found based on the the mass and stiffness matrix adjustments at the previous iteration, $\Delta \boldsymbol{M}^{(n-1)}$ and $\Delta \boldsymbol{K}^{(n-1)}$. Then, the mass and stiffness matrices are corrected based on the newly expanded mode shapes. This process is detailed next.

After the correction of the mass and stiffness matrices, the functionals J and K, have been minimized. This has forced the first terms of Eqs. (17) and (18) to some small values. These values are defined as the complex residuals

$$\boldsymbol{R}_i^{\text{real}} = [-(\sigma_i^{E2} + \omega_i^{E2})\boldsymbol{M}^U + \boldsymbol{K}^U] \begin{bmatrix} \Psi_{iM}^{\text{real } E} \\ \Psi_{iNM}^{\text{real } E} \end{bmatrix} \qquad \text{for} \qquad i = 1, \ldots, c$$
$$\boldsymbol{R}_i^{\text{imag}} = [-(\sigma_i^{E2} + \omega_i^{E2})\boldsymbol{M}^U + \boldsymbol{K}^U] \begin{bmatrix} \Psi_{iM}^{\text{imag } E} \\ \Psi_{iNM}^{\text{imag } E} \end{bmatrix} \quad (21)$$

For lightly damped structures, the correction of the mass and stiffness matrices based on the minimization of these residuals is valid because the real and imaginary components of the complex modes should be nearly parallel with the normal modes of the system. In addition, the moduli of the complex eigenvalues should be very close to the associated undamped normal frequencies.

1. *Mode Shape Expansion*

The first part of the iterative process updating the mass and stiffness matrices is the expansion of the experimental complex mode shapes. Taking the first variation of the functionals (19) and (20) produces a system of equations to be solved for the mode expansions $\Psi_{NM}^{E(n)}$,

$$\frac{\partial J_i(\boldsymbol{K}^{U(n-1)}, \boldsymbol{M}^{U(n-1)})}{\partial \Psi_{NM}^{\text{real } E}} = 0$$
$$\frac{\partial K_i(\boldsymbol{K}^{U(n-1)}, \boldsymbol{M}^{U(n-1)})}{\partial \Psi_{NM}^{\text{imag } E}} = 0 \qquad \text{for} \qquad i = 1, \ldots, c \quad (22)$$

The mass and stiffness matrices $\boldsymbol{K}^U$ and $\boldsymbol{M}^U$ are partitioned into measured and unmeasured components

$$\boldsymbol{K}^U = \begin{bmatrix} \boldsymbol{K}_{M,M}^U & \boldsymbol{K}_{M,NM}^U \\ \boldsymbol{K}_{NM,M}^U & \boldsymbol{K}_{NM,NM}^U \end{bmatrix}$$
$$\boldsymbol{M}^U = \begin{bmatrix} \boldsymbol{M}_{M,M}^U & \boldsymbol{M}_{M,NM}^U \\ \boldsymbol{M}_{NM,M}^U & \boldsymbol{M}_{NM,NM}^U \end{bmatrix} \quad (23)$$

The ith impedance matrix is defined as

$$\boldsymbol{Z}_i^U = \begin{bmatrix} \boldsymbol{Z}_{iM,M}^U & \boldsymbol{Z}_{iM,NM}^U \\ \boldsymbol{Z}_{iNM,M}^U & \boldsymbol{Z}_{iNM,NM}^U \end{bmatrix} = \boldsymbol{K}^U - (\sigma_i^{E2} + \omega_i^{E2})\boldsymbol{M}^U \qquad \text{for} \qquad i = 1, \ldots, c \quad (24)$$

Using the definition of $\boldsymbol{Z}^U$, the first variations given in Eq. (22) yield a system of equations for the unmeasured mode shape components:

$$\boldsymbol{A}_i^{(n)} \Psi_{iNM}^{\text{real } E(n)} = -\boldsymbol{b}_i^{\text{real}(n)}$$
$$\boldsymbol{A}_i^{(n)} \Psi_{iNM}^{\text{imag } E(n)} = -\boldsymbol{b}_i^{\text{imag}(n)} \qquad \text{for} \qquad i = 1, \ldots, c \quad (25)$$

where

$$\boldsymbol{A}_i^{(n)} = \left[\boldsymbol{Z}_{i\,NM,NM}^{U(n-1)}\right]^T\left[\boldsymbol{Z}_{i\,NM,NM}^{U(n-1)}\right] + \left[\boldsymbol{Z}_{i\,M,NM}^{U(n-1)}\right]^T\left[\boldsymbol{Z}_{i\,M,NM}^{U(n-1)}\right]$$

$$\boldsymbol{b}_i^{\text{real}\,(n)} = \left[\left[\boldsymbol{Z}_{i\,NM,NM}^{U(n-1)}\right]^T\left[\boldsymbol{Z}_{i\,M,NM}^{U(n-1)}\right]^T + \left[\boldsymbol{Z}_{i\,M,NM}^{U(n-1)}\right]^T\left[\boldsymbol{Z}_{i\,M,M}^{U(n-1)}\right]\right]\boldsymbol{\Psi}_{iM}^{\text{real}\,E}$$

$$\boldsymbol{b}_i^{\text{imag}\,(n)} = \left[\left[\boldsymbol{Z}_{i\,NM,NM}^{U(n-1)}\right]^T\left[\boldsymbol{Z}_{i\,M,NM}^{U(n-1)}\right]^T + \left[\boldsymbol{Z}_{i\,M,NM}^{U(n-1)}\right]^T\left[\boldsymbol{Z}_{i\,M,M}^{U(n-1)}\right]\right]\boldsymbol{\Psi}_{iM}^{\text{imag}\,E} \tag{26}$$

The solution to Eq. (25) produces the expansion for each mode i. Note that $\boldsymbol{A}_i^{(n)}$ is a square matrix with the size of the unmeasured degrees of freedom and appears in both the real and imaginary mode equation. Therefore, the same factorization of $\boldsymbol{A}_i^{(n)}$ can be used for both the real and imaginary expansion of mode i. The factorization of $\boldsymbol{A}_i^{(n)}$ is the most computationally expensive part of the mode expansion. Note that $\boldsymbol{Z}_{i\,NM,NM}^{U(n-1)}$ has the same the same sparsity pattern as the stiffness matrix $\boldsymbol{K}_{NM,NM}^{U}$. However, when the matrix $\boldsymbol{A}_i^{(n)}$ is computed, this sparsity pattern is destroyed. For this reason, in practice, the left-hand side of Eq. (25) is not explicitly formed and factored. Instead, the Woodbury formula is applied leading to greater computational efficiency.[1,28] For large problems, the computational cost of the mode expansion is less than the cost of factoring the stiffness matrix $\boldsymbol{K}$.

2. Updating of Mass and Stiffness Matrices

Following the expansion of the complex modes, the mass and stiffness matrices are corrected. The update matrices at the current iteration $\Delta\boldsymbol{K}^{(n)}$ and $\Delta\boldsymbol{M}^{(n)}$ are to be determined based on the current mode expansions $\boldsymbol{\Psi}_{NM}^{E(n)}$ and the update matrices at the previous iteration $\Delta\boldsymbol{K}^{(n-1)}$ and $\Delta\boldsymbol{M}^{(n-1)}$. The partial derivative terms in Eqs. (9) and (10) are defined as the sensitivity matrices

$$\boldsymbol{s}_k^{e,(n)} = \frac{\partial \boldsymbol{k}_e(\boldsymbol{p}^{(n)})}{\partial p_k}$$
$$\boldsymbol{t}_k^{e,(n)} = \frac{\partial \boldsymbol{m}_e(\boldsymbol{p}^{(n)})}{\partial p_k} \tag{27}$$

With the update matrices expressed in terms of the design parameters, the only unknowns are the parameter adjustments $\delta\boldsymbol{p}$. Using the expanded mode shapes and taking the first variation of the functionals (19) and (20) with respect to the design parameter adjustments yields a system of algebraic linear equations. The equations from the real and imaginary functionals can be stacked together in a rectangular matrix,

$$\boldsymbol{B}^{(n)}\delta\boldsymbol{p}^{(n)} = -\boldsymbol{R}^{(n-1)} \tag{28}$$

where

$$\boldsymbol{R}^{(n-1)} = \begin{bmatrix} \boldsymbol{R}_1^{\text{real}\,(n-1)} \\ \vdots \\ \boldsymbol{R}_c^{\text{real}\,(n-1)} \\ \boldsymbol{R}_1^{\text{imag}\,(n-1)} \\ \vdots \\ \boldsymbol{R}_c^{\text{imag}\,(n-1)} \end{bmatrix} \tag{29}$$

and

$$\boldsymbol{B}^{(n)} = \begin{bmatrix} \boldsymbol{z}_{1,1}^{1,(n)}\boldsymbol{L}^1\boldsymbol{\Psi}_1^{\text{real}\,E(n)} & \cdots & \boldsymbol{z}_{N_p^{(N_e)},1}^{N_e,(n)}\boldsymbol{L}^{N_e}\boldsymbol{\Psi}_1^{\text{real}\,E(n)} \\ \vdots & \ddots & \vdots \\ \boldsymbol{z}_{1,c}^{1,(n)}\boldsymbol{L}^1\boldsymbol{\Psi}_c^{\text{real}\,E(n)} & \cdots & \boldsymbol{z}_{N_p^{(N_e)},c}^{N_e,(n)}\boldsymbol{L}^{N_e}\boldsymbol{\Psi}_c^{\text{real}\,E(n)} \\ \boldsymbol{z}_{1,1}^{1,(n)}\boldsymbol{L}^1\boldsymbol{\Psi}_1^{\text{imag}\,E(n)} & \cdots & \boldsymbol{z}_{N_p^{(N_e)},1}^{N_e,(n)}\boldsymbol{L}^{N_e}\boldsymbol{\Psi}_1^{\text{imag}\,E(n)} \\ \vdots & \ddots & \vdots \\ \boldsymbol{z}_{1,c}^{1,(n)}\boldsymbol{L}^1\boldsymbol{\Psi}_c^{\text{imag}\,E(n)} & \cdots & \boldsymbol{z}_{N_p^{(N_e)},c}^{N_e,(n)}\boldsymbol{L}^{N_e}\boldsymbol{\Psi}_c^{\text{imag}\,E(n)} \end{bmatrix} \tag{30}$$

with

$$\boldsymbol{z}_{k,i}^{e,(n)} = (\boldsymbol{s}_k^{e,(n)} - (\sigma_i^{E\,2} + \omega_i^{E\,2})\boldsymbol{t}_k^{e,(n)}) \tag{31}$$

$$\delta\boldsymbol{p}^{(n)} = \left[\delta p_1^{1,(n)} \quad \delta p_2^{1,(n)} \quad \cdots \quad \delta p_{N_p^{(1)}}^{1,(n)} \quad \cdots \quad \delta p_{N_p^{(N_e)}}^{N_e,(n)}\right]^T \tag{32}$$

The localization operator $\boldsymbol{L}^{(e)}$ extracts from the vector following, in this case $\boldsymbol{\Psi}^{\text{real}\,E(n)}$ or $\boldsymbol{\Psi}^{\text{imag}\,E(n)}$, those degrees of freedom that are attached to the nodes of FE e. This yields a vector or reduced length equal to the number of degrees of freedom attached to element e. Thus, $\boldsymbol{z}^{e,(n)}$ is multiplied by the relevant entries of the complex mode shapes. Each column of $\boldsymbol{B}^{(n)}$ corresponds to a particular design parameter. A block of $N_p^{(e)}$ columns contains all of the design parameters of FE e. If the total number of analytic degrees of freedom is N_{dof}, then the number of rows of $\boldsymbol{B}^{(n)}$ is $2 \times N_{\text{dof}} \times c$. Notice that the upper block of $\boldsymbol{B}^{(n)}$ corresponds to the real portion of the complex modes, whereas the lower block corresponds to the imaginary portion. As written, the solution vector to the system of equations contains every design parameter of every element. In practice, only a small subset of these design parameters would be corrected at any given iteration. Utilizing zooming,[1] as discussed earlier, allows the algorithm to select design parameters related to the dominant error locations of the model. The correction system for the parameter adjustments is overdetermined, with equations arising from both the real and imaginary functionals. An SVD factorization is used to obtain the design parameter adjustments. Using these parameter adjustments, the updated mass and stiffness matrices can be constructed.

C. Updating of Damping Matrix

The updating of the mass and stiffness matrices has made the residuals $\boldsymbol{R}^{\text{real}}$ and $\boldsymbol{R}^{\text{imag}}$ as small as possible. In the second step of the process, the damping matrix is corrected using the updated mass and stiffness matrices and the complex mode shapes. Using the updated matrices, expanded modes, and residuals in Eqs. (17) and (18) gives

$$\boldsymbol{R}_i^{\text{real}} + \left[2\sigma_i^{E\,2}\boldsymbol{M}^U + \sigma_i^E(\boldsymbol{D}^A + \Delta\boldsymbol{D})\right]\boldsymbol{\Psi}_i^{\text{real}\,E} - \left[2\sigma_i^E\omega_i^E\boldsymbol{M}^U + \omega_i^E(\boldsymbol{D}^A + \Delta\boldsymbol{D})\right]\boldsymbol{\Psi}_i^{\text{imag}\,E} = 0 \qquad i = 1, \ldots, c \tag{33}$$

$$\boldsymbol{R}_i^{\text{imag}} + \left[2\sigma_i^{E\,2}\boldsymbol{M}^U + \sigma_i^E(\boldsymbol{D}^A + \Delta\boldsymbol{D})\right]\boldsymbol{\Psi}_i^{\text{imag}\,E} + \left[2\sigma_i^E\omega_i^E\boldsymbol{M}^U + \omega_i^E(\boldsymbol{D}^A + \Delta\boldsymbol{D})\right]\boldsymbol{\Psi}_i^{\text{real}\,E} = 0 \qquad i = 1, \ldots, c \tag{34}$$

The problem of updating the damping matrix is to find the change to the damping matrix $\Delta\boldsymbol{D}$ such that Eqs. (33) and (34) are satisfied. Note the only unknown is $\Delta\boldsymbol{D}$ because the updated mass and stiffness matrices $\boldsymbol{M}^U$ and $\boldsymbol{K}^U$, as well as the mode expansions $\boldsymbol{\Psi}^E$, are assumed to be known from the first step of the process. The updating problem is, in general, rectangular and is formulated as the minimization of the following functionals:

$$\bar{J}_i = \left\| \boldsymbol{R}_i^{\text{real}} + \left[2\sigma_i^{E\,2}\boldsymbol{M}^U + \sigma_i^E(\boldsymbol{D}^A + \Delta\boldsymbol{D})\right]\boldsymbol{\Psi}_i^{\text{real}\,E} - \left[2\sigma_i^E\omega_i^E\boldsymbol{M}^U + \omega_i^E(\boldsymbol{D}^A + \Delta\boldsymbol{D})\right]\boldsymbol{\Psi}_i^{\text{imag}\,E} \right\|_2 \qquad i = 1, \ldots, c \tag{35}$$

$$\bar{K}_i = \left\| \boldsymbol{R}_i^{\text{imag}} + \left[2\sigma_i^{E\,2}\boldsymbol{M}^U + \sigma_i^E(\boldsymbol{D}^A + \Delta\boldsymbol{D})\right]\boldsymbol{\Psi}_i^{\text{imag}\,E} + \left[2\sigma_i^E\omega_i^E\boldsymbol{M}^U + \omega_i^E(\boldsymbol{D}^A + \Delta\boldsymbol{D})\right]\boldsymbol{\Psi}_i^{\text{real}\,E} \right\|_2 \qquad i = 1, \ldots, c \tag{36}$$

Although the updated stiffness matrix $\boldsymbol{K}^U$ does not appear explicitly, it enters into the functionals via the complex residuals $\boldsymbol{R}$. The damping update matrix $\Delta\boldsymbol{D}$ is built using a Taylor expansion with respect to the design parameters $\boldsymbol{p}$,

$$\Delta\boldsymbol{D} = \boldsymbol{D}(\boldsymbol{p} + \delta\boldsymbol{p}) - \boldsymbol{D}(\boldsymbol{p}) \approx \left[\frac{\partial \boldsymbol{D}(\boldsymbol{p})}{\partial \boldsymbol{p}}\right]\delta\boldsymbol{p} \tag{37}$$

As stated earlier, in this method, the damping matrix can be built using any user-defined model. It could be built at the element level, or could be built using some other model. The case where damping

is built at the element level will be considered. For this case, the assembly property of FEs can be used so that

$$\Delta \boldsymbol{D} \approx \sum_{e}^{N_e} \sum_{k}^{N_p^{(e)}} \left[\frac{\partial \boldsymbol{d}_e(\boldsymbol{p})}{\partial p_k} \right] \delta p_k \tag{38}$$

The derivative term in Eq. (38) is defined as the damping sensitivity matrix

$$\boldsymbol{sd}_k^e = \frac{\partial \boldsymbol{d}_e(\boldsymbol{p})}{\partial p_k} \tag{39}$$

We define the following combination mode vectors:

$$\begin{aligned} \boldsymbol{Y}_i^{\text{real}} &= \left[-\sigma_i^E \boldsymbol{\Psi}_i^{\text{real } E} + \omega_i^E \boldsymbol{\Psi}_i^{\text{imag } E} \right] \\ \boldsymbol{Y}_i^{\text{imag}} &= \left[-\sigma_i^E \boldsymbol{\Psi}_i^{\text{imag } E} - \omega_i^E \boldsymbol{\Psi}_i^{\text{real } E} \right] \end{aligned} \qquad i = 1, \ldots, c \tag{40}$$

and the following modified complex residuals:

$$\begin{aligned} \bar{\boldsymbol{R}}_i^{\text{real}} &= \boldsymbol{R}_i^{\text{real}} + 2\sigma_i^{E\,2} \boldsymbol{M}^U \boldsymbol{\Psi}_i^{\text{real } E} - 2\sigma_i^E \omega_i^E \boldsymbol{M}^U \boldsymbol{\Psi}_i^{\text{imag } E} \\ \bar{\boldsymbol{R}}_i^{\text{imag}} &= \boldsymbol{R}_i^{\text{imag}} + 2\sigma_i^{E\,2} \boldsymbol{M}^U \boldsymbol{\Psi}_i^{\text{imag } E} + 2\sigma_i^E \omega_i^E \boldsymbol{M}^U \boldsymbol{\Psi}_i^{\text{real } E} \end{aligned} \qquad i = 1, \ldots, c \tag{41}$$

For a damping model, which depends only linearly on the design parameters, using the definitions (40) and (41) allows us to write the functionals (35) and (36) in a very simple form:

$$\bar{J}_i = \left\| \bar{\boldsymbol{R}}_i^{\text{real}} - \Delta \boldsymbol{D}\, \boldsymbol{Y}_i^{\text{real}} \right\|_2 \qquad i = 1, \ldots, c \tag{42}$$

$$\bar{K}_i = \left\| \bar{\boldsymbol{R}}_i^{\text{imag}} - \Delta \boldsymbol{D}\, \boldsymbol{Y}_i^{\text{imag}} \right\|_2 \qquad i = 1, \ldots, c \tag{43}$$

In this case, no iteration or initial conditions of the damping matrix are required. The only unknowns are the design parameter adjustments $\delta \boldsymbol{p}$ that are used to build $\boldsymbol{D}^U = \Delta \boldsymbol{D}$. The correction system is obtained by equating the first variation of the functionals to zero:

$$\begin{aligned} \frac{\partial \bar{J}_i(\boldsymbol{Y}_i^{\text{real}}, \bar{\boldsymbol{R}}_i^{\text{real}})}{\partial \delta \boldsymbol{p}} &= 0 \\ \frac{\partial \bar{K}_i(\boldsymbol{Y}_i^{\text{imag}}, \bar{\boldsymbol{R}}_i^{\text{imag}})}{\partial \delta \boldsymbol{p}} &= 0 \end{aligned} \qquad i = 1, \ldots, c \tag{44}$$

This yields a system of algebraic equations to be solved for the design parameter adjustments $\delta \boldsymbol{p}$. The equations arising from the real and imaginary functionals are stacked together in a rectangular system,

$$\boldsymbol{C} \delta \boldsymbol{p} = \bar{\boldsymbol{R}} \tag{45}$$

where

$$\bar{\boldsymbol{R}} = \begin{bmatrix} \bar{\boldsymbol{R}}_1^{\text{real}} \\ \vdots \\ \bar{\boldsymbol{R}}_c^{\text{real}} \\ \bar{\boldsymbol{R}}_1^{\text{imag}} \\ \vdots \\ \bar{\boldsymbol{R}}_c^{\text{imag}} \end{bmatrix} \tag{46}$$

and

$$\boldsymbol{C} = \begin{bmatrix} \boldsymbol{sd}_1^1 \boldsymbol{L}^1 \boldsymbol{Y}_1^{\text{real}} & \cdots & \boldsymbol{sd}_{N_p^{(Ne)}}^{N_e} \boldsymbol{L}^{N_e} \boldsymbol{Y}_1^{\text{real}} \\ \vdots & \ddots & \vdots \\ \boldsymbol{sd}_1^1 \boldsymbol{L}^1 \boldsymbol{Y}_c^{\text{real}} & \cdots & \boldsymbol{sd}_{N_p^{(Ne)}}^{N_e} \boldsymbol{L}^{N_e} \boldsymbol{Y}_c^{\text{real}} \\ \boldsymbol{sd}_1^1 \boldsymbol{L}^1 \boldsymbol{Y}_1^{\text{imag}} & \cdots & \boldsymbol{sd}_{N_p^{(Ne)}}^{N_e} \boldsymbol{L}^{N_e} \boldsymbol{Y}_1^{\text{imag}} \\ \vdots & \ddots & \vdots \\ \boldsymbol{sd}_1^1 \boldsymbol{L}^1 \boldsymbol{Y}_c^{\text{imag}} & \cdots & \boldsymbol{sd}_{N_p^{(Ne)}}^{N_e} \boldsymbol{L}^{N_e} \boldsymbol{Y}_c^{\text{imag}} \end{bmatrix} \tag{47}$$

with

$$\delta \boldsymbol{p} = \left[\delta p_1^1 \quad \delta p_2^1 \quad \cdots \quad \delta p_{N_p^{(1)}}^1 \quad \cdots \quad \delta p_{N_p^{(Ne)}}^{N_e} \right]^T \tag{48}$$

As before, $\boldsymbol{L}^e$ is the localization operator that extracts degrees of freedom attached to nodes of element e. The number of columns of $\boldsymbol{C}$ is the number of damping design parameters in the model. There are $2 \times N_{\text{dof}} \times c$ rows in the matrix. The upper block of $\boldsymbol{C}$ derives from the variation of the real functional, whereas the lower block is the result of the variation of the imaginary functional. Each column of $\boldsymbol{C}$ corresponds to a particular damping design parameter. The system of equations is overdetermined, and so an SVD factorization is used to determine the design parameters. The damping matrix $\boldsymbol{D}^U$ can then be assembled.

The modified SVD solver and dimensionless procedure developed by Hemez and Farhat[27] can be used to help bypass numerical difficulties associated with poor scaling between different damping effects. This dimensionless procedure is equivalent to preconditioning each column of $\boldsymbol{C}$, by scaling each coefficient by the norm of the column.

This system of equations assumes that each design parameter is associated with a particular element. If multiple elements are constrained to use the same parameter, then summation terms are introduced. In this case, each column of $\boldsymbol{C}$ would contain an assembly of all nonzero sensitivity matrices with respect to that parameter, as opposed to a single element sensitivity matrix. Thus, the size of the correction system can be reduced by using a simple damping model. For instance, all longeron elements in a truss structure might be constrained to have the same material damping parameters.

This process allows the damping matrix to be determined by finding the optimum values of design parameters within a user-defined model. The two step arrangement allows computation of the damping matrix to be decoupled from the SB-EBE mass and stiffness update.

IV. Results from Test Problems

A. Ten-Degree-of-Freedom Problem

The proposed extension is first tested with the FE updating of a 10-degree-of-freedom test problem. This problem examines the effect of the amount of structural damping upon updating of the FE mass and stiffness matrices and upon the computation of the damping matrix. The analytic model used to create the simulated data comprises a set of 10 spring and dashpot units. This is shown in Fig. 1. The values of the spring coefficients, dashpot coefficients, and discrete masses are set to

$$\begin{aligned} k_1 = k_2 = \ldots = k_9 = k_{10} &= 1.0 \times 10^6 \\ m_1 = m_2 = \ldots = m_9 = 2m_{10} &= 0.1 \\ [d_1, d_2, \ldots, d_9, d_{10}] &= d \\ \times [5.0, 4.5, 4.0, 3.5, 3.0, 2.5, 2.0, 1.5, 1.0, 0.5] & \end{aligned} \tag{49}$$

where d is an adjustable scaling factor. During updating, half of the 10 degrees of freedom are assumed to be measured. Because the values of the dashpots decrease linearly across the structure, nonproportional damping is created. The FE model is composed of 10 truss elements, each with element level stiffness proportional damping. Modeling errors are introduced by reducing the modulus of the second element and the density of the third element by 5%. Thus, there is a simultaneous mass and stiffness perturbation. Complex modes 1–5 of the available 10 are used for the update. These modes are chosen because they involve motion of the masses near the fixation and allow the perturbed elements to be observable.

The two-step procedure is applied for a 3% damping level in the simulated data. These results are shown in Fig. 2. The update of

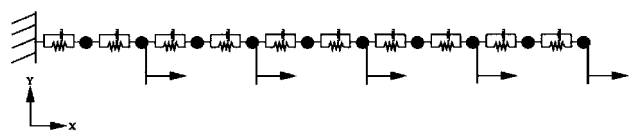

Fig. 1 Structure with 10 degrees of freedom.

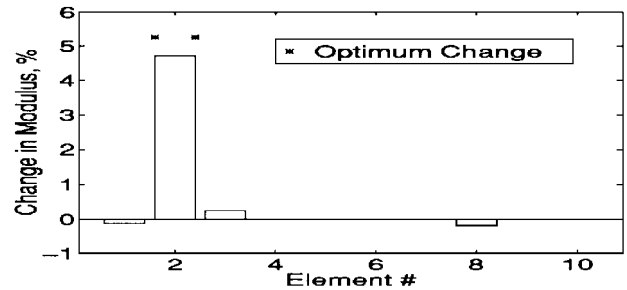

Adjustment of Young's modulus

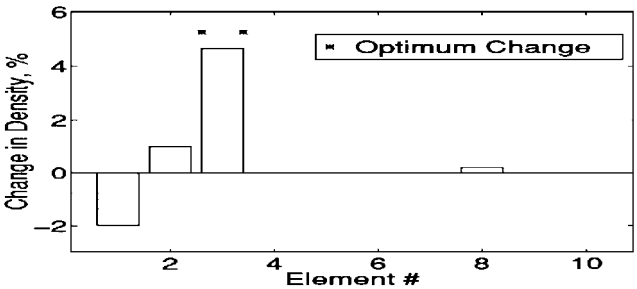

Adjustment of density

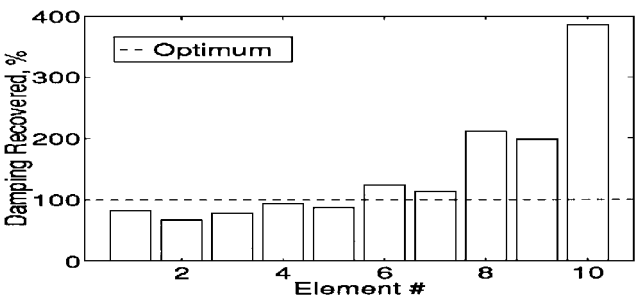

Calculation of damping

Fig. 2 Updating results at 3% damping.

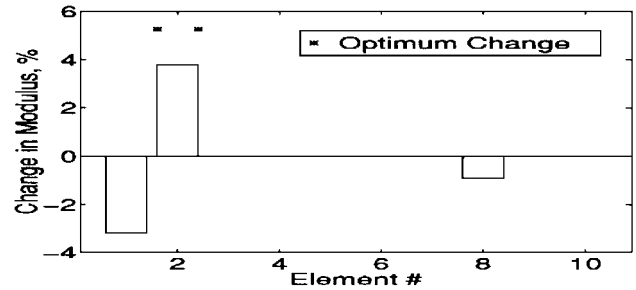

Adjustment of Young's modulus

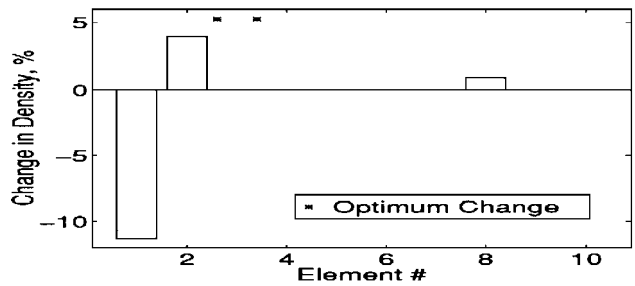

Adjustment of density

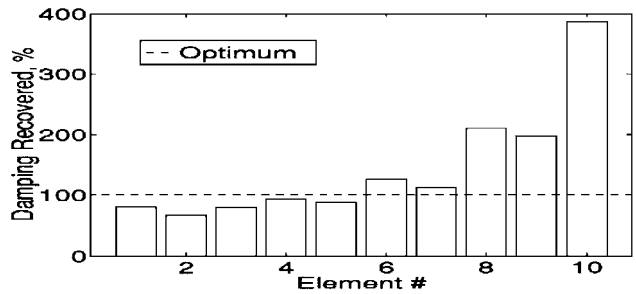

Calculation of damping

Fig. 3 Updating results at 6% damping.

the mass and stiffness matrices shows good results; the change in the modulus and density for the incorrect elements is greater than the change in the undamaged elements. Thus, the algorithm is able to correct simultaneous errors in the mass and stiffness of elements two and three. The correction of the damping matrix also shows reasonable results, as the final values of the dashpots are close to the desired value for most elements. However, the amount of damping near the fixed end of the structure is underestimated, whereas toward the free end of the structure, damping is overestimated. This is due to the least squares nature of the solution. In addition, the modes used for the update are dominated by the motion of the masses near the fixation, resulting in less information available about the springs, masses, and dashpots at the free end of the structure.

The procedure is then applied for increasing levels of damping in the simulated data. As the amount of damping increases, the quality of the mass and stiffness update begins to deteriorate. At a damping level of approximately 6%, the damaged elements are not satisfactorily located. At this high level of damping, the complex modes are not sufficiently parallel to the normal modes. The results of the updating procedure for a 6% damping level are shown in Fig. 3. Note that, although the stiffness error in element two is corrected, a large adjustment is introduced in an adjacent element. The mass error in element three is not corrected, whereas there are large adjustments in other elements. Interestingly, the behavior of the damping matrix computation shows virtually no change as compared to the previous results. The percent of the optimum dashpot value recovered appears almost identical to the results at the 3% damping level. This similarity is partially due to the fact that the dashpots are equivalent to element level stiffness proportional damping and, thus, are not affected by the large inaccuracies in the mass matrix. These damping results suggest the possibility of a good update of the damping matrix at high damping levels if the mass and stiffness portion of the update could be improved.

Tests show that the ability to localize the mass and stiffness errors relies heavily on both the real- and imaginary-derived equations for the parameter adjustments. Removing either component destroys the quality of the update. As expected, tests with a globally proportionally damped structure provide optimum results compatible with the original SB-EBE procedure.

In summary, the proposed extension is tested with a 10-degree-of-freedom system. Reasonable results are obtained for damping levels of approximately 3%. This illustrates the potential performance of the procedure for the updating of lightly damped structures.

B. Simulation Problem for a Real Truss Structure

This example shows the results of applying the algorithm to a realistic test problem, in this case a truss structure. The structure consists of eight $\frac{1}{2}$-m bays and 36 joints. There are five 1-lb and three 5-lb masses, for a total of eight concentrated masses. This makes the nonstructural mass approximately 50% of the total mass. The lowest modes of the structure are dominated by the vibration of the large concentrated masses. This gives highly localized modal behavior that is representative of large space structures. The three translational degrees of freedom are measured at each joint, for a total of 108 sensor locations. This simulated problem is based on a real experimental truss used in damage detection experiments. However, preloading of the members in the real truss was effective in reducing the damping of the structure to the order of $\frac{1}{10}$%. In the simulated data, the modal damping level is increased to a level of approximately 3%. The lower frequency modes of the structure involve large deformations of the members near the concentrated masses. The presence of damping creates complex modes that do not have a one to one correlation with the undamped normal modes of the structure. A diagram of this structure is shown in Fig. 4.

Each longeron of the truss is discretized by five Euler–Bernoulli beam FEs. Damping in the model is built using an element level

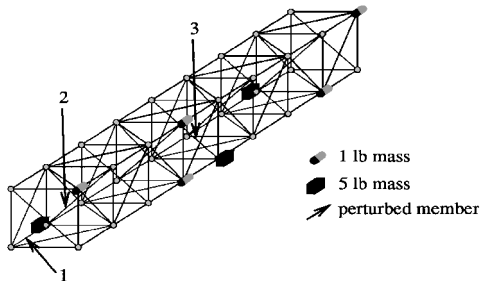

Fig. 4 Truss structure.

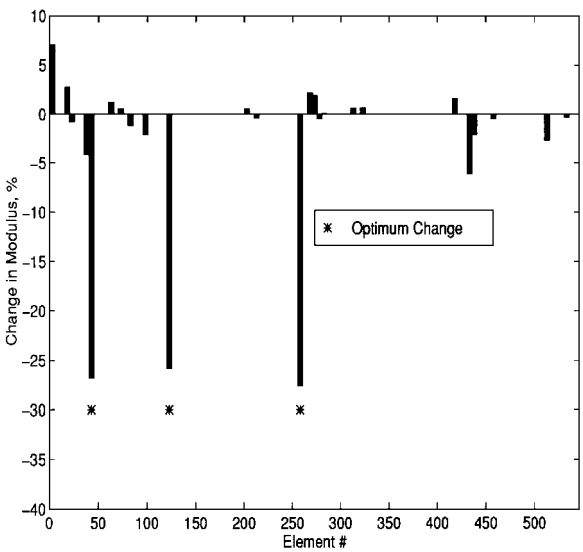

Fig. 5 Adjusted Young's moduli: updating of stiffness matrix.

proportional damping scheme. Note that this is not equivalent to global proportional damping, inasmuch as element level damping coefficients are allowed to vary independently. The building of the damping matrix at the element level is written as

$$\boldsymbol{D} = \sum_{e=1}^{N_e} \alpha^{(e)} \boldsymbol{k}_e + \beta^{(e)} \boldsymbol{m}_e \tag{50}$$

In total, the FE model contains 472 nodes and 545 elements. This gives 2832 analytical degrees of freedom of which 108 (approximately 4%) are measured. Free-free boundary conditions are used throughout.

Errors are introduced by perturbing the stiffness of the three longerons indicated in Fig. 4. Young's moduli of the FEs representing these longerons are increased by 43%. Because these members are near two of the concentrated masses that dominate the modal behavior, they store a larger percentage of the strain energy than elements distant from the masses. Thus, they are observable by the updating algorithm. In this updating problem, we wish to apply the proposed SB-EBE extension to correct the stiffness modeling errors and compute the damping matrix using the simulated experimental complex modes.

During updating, the algorithm is set to select the elements to be corrected using the SB-EBE zooming procedure. For this problem, only Young's moduli are altered, and so the mass matrix is unchanged. Note that the element stiffness matrix of the beam depends only linearly on the modulus, so that large adjustments are valid. A maximum of 100 elements, or 20 longerons, are corrected at each iteration. All elements comprising a given longeron are constrained to have the same adjustment. Six complex modes are used for the update (1, 2, 3, 4, 14, 20). Thus, the maximum size of the correction system $\boldsymbol{B}$ [in Eq. (30)] is $20 \times 33{,}984$. The chosen modes involve motion of the large masses and allow the perturbed elements to be observable. The adjustments of the element moduli after 150 iterations are shown in Fig. 5. The algorithm has satisfactorily located the perturbed elements, as their moduli are reduced more than the

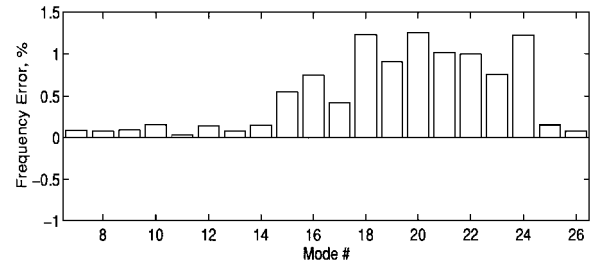

Before updating

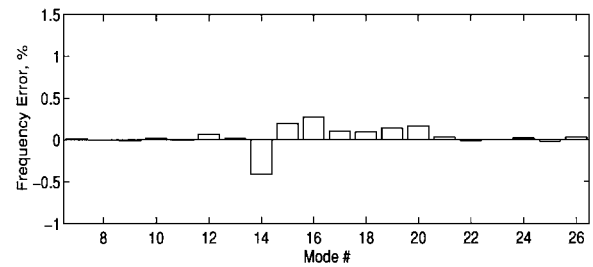

After updating

Fig. 6 Errors between model and experimental frequencies: undamped frequency errors.

adjustment to the surrounding unperturbed members. The moduli of the perturbed longerons are brought back near their optimum values. A few longerons in other areas of the structure are also slightly adjusted.

The frequency errors between the model and experimental data can be used to examine the quality of the update. The undamped frequency errors, before and after the updating of the stiffness matrix, are shown in Fig. 6 for the first 20 normal elastic modes. Before updating, the higher modulus of the perturbed elements introduces errors in the normal frequencies of the model that are as high as $1\frac{1}{2}\%$. After the stiffness adjustment, the frequency errors are reduced to less than $\frac{1}{2}\%$. Thus, the procedure improves the undamped frequencies of the model, even though the updating procedure uses damped complex modes.

Following the updating of the stiffness matrix, the damping matrix is calculated. As already discussed, an element level proportional damping model is used. To reduce the size of the problem, damping coefficients are not computed for all elements. Instead, the number of parameters is reduced by forcing multiple elements to use the same element level proportional damping coefficients. All elements attached to a particular joint are forced to have the same set of element proportional damping coefficients. However, each different joint has an independent set of damping coefficients. All elements not directly attached to joints are given the same damping parameters, representing material damping or other effects. Because, in many structures, joints dominate the damping behavior, the damping model is a reasonable approximation of what might be applied in the modeling of real structures. Because there are 36 joints, there is a total 74 independent damping parameters. Therefore, the size of $\boldsymbol{C}$ in Eq. (47) is 74 by 33,984. Note, that this is a linear damping model, and so no initial conditions are required for the damping matrix.

Using the updated stiffness matrix and expanded mode shapes, the damping matrix is constructed. With the newly computed damping matrix, the complex eigenvalues are computed and compared against experiment. This is shown in Fig. 7. Note that the mode numbering is not the same as for the undamped modes. The errors in the imaginary parts of the eigenvalues (damped frequencies) are all less than $\frac{1}{2}\%$ for the first 20 modes. The real part of the eigenvalue contains errors of a few percent, with a few modes containing errors as high as 6%. As only six complex modes were used in the update, the results for the remaining modes show the predictive behavior of the method. The real part of the eigenvalue is representative of the amount of damping in a given mode. A comparison of the estimated damping ratios of the experimental data vs the model is shown in Fig. 8. Note that the two graphs show similar behavior, with the same modes corresponding

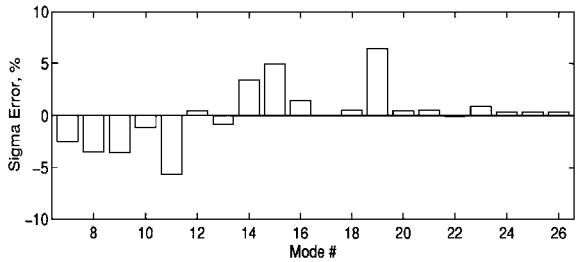

Real parts

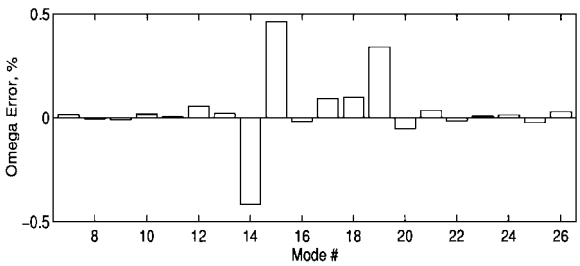

Imaginary parts

Fig. 7 Updated damped model vs experiment: errors of eigenvalues.

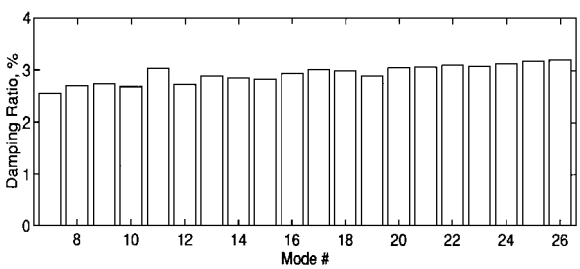

Experimental damping ratios

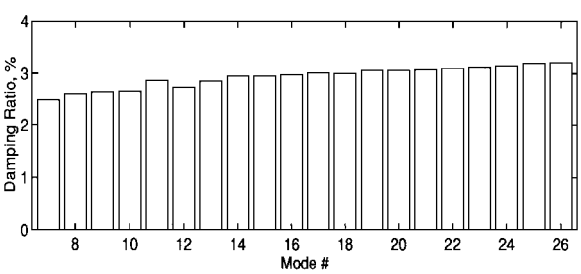

Model damping ratios

Fig. 8 Damping ratios of model vs experiment.

to the highest and lowest levels of damping. Together, the complex eigenvalues and damping ratios show the correct physical behavior of the computed damping matrix. The algorithm gives reasonable results for the computation of the system damping in a structure with approximately 3% damping.

The results from the update of the stiffness matrix and the update of the damping matrix show reasonable performance of the proposed procedure for a realistic lightly damped structure using complex modes.

V. Conclusion

An extension to the SB-EBE method for updating the FE models of lightly damped structures using experimentally measured complex modes is presented. This proposed extension consists of a two-step procedure. First, an iterative step expands the experimental mode shapes and updates the mass and stiffness matrices. This is done through the minimization of a set of dynamic residuals. The update of the mass and stiffness matrices is built through changes in model design parameters. This maintains the connectivity of the model and gives an update based on the physical sources of the modeling errors. For mass and stiffness matrices that depend linearly on the design parameters, large perturbations are acceptable. Following the update of the mass and stiffness matrices, a second step updates the damping matrix. This step utilizes the previously expanded modes shapes and the updated mass and stiffness matrices. The remainder of the dynamic residuals from the first step of the process are absorbed during the update of the damping matrix. The update of the damping matrix also is built through the adjustment of design parameters. For a damping matrix that depends linearly on the parameters, no iteration or initial conditions are required. Thus, for such models, the computational cost of updating a damped system is only slightly higher than that of updating the associated undamped system. Two simulation examples are presented and discussed. In these examples, satisfactory updating of the mass, stiffness, and damping matrices is demonstrated. These results illustrate the potential of the proposed extension to the SB-EBE procedure for the updating of damped structures through the use of complex modes.

References

[1]Hemez, F. M., and Farhat, C., "Structural Damage Detection via a Finite Element Model Updating Methodology," *Modal Analysis*, Vol. 10, No. 3, 1995, pp. 152–166.

[2]Farhat, C., and Hemez, F. M., "Updating Finite Element Dynamical Models Using an Element-by-Element Sensitivity Methodology," *AIAA Journal*, Vol. 31, No. 9, 1993, pp. 1702–1711.

[3]Hemez, F. M., "Theoretical and Experimental Correlation Between Finite Element Models and Modal Tests in the Context of Large Flexible Space Structures," Ph.D. Dissertation, Center for Aerospace Structures, Rept. CU-CAS-93-18, Univ. of Colorado, Boulder, CO, July 1993.

[4]Baruch, M., "Optimization Procedure to Correct Stiffness and Flexibility Matrices Using Vibration Tests," *AIAA Journal*, Vol. 16, No. 11, 1978, pp. 1209, 1210.

[5]Berman, A., and Nagy, E. J., "Improvement of a Large Analytical Model Using Test Data," *AIAA Journal*, Vol. 21, No. 8, 1983, pp. 1168–1173.

[6]Caesar, B., "Update and Identification of Dynamic Mathematical Models," *Proceedings of the 1st UC/SEM International Modal Analysis Conference* (Orlando, FL), Society of Experimental Mechanics, Bethel, CT, 1983, pp. 394–401.

[7]Kabe, A. M., "Stiffness Matrix Adjustment Using Mode Data," *AIAA Journal*, Vol. 23, No. 9, 1985, pp. 1431–1436.

[8]Smith, S. W., and Beattie, C. A., "Secant-Method Adjustment for Structural Models," *AIAA Journal*, Vol. 29, No. 1, 1991, pp. 119–126.

[9]Chen, J. C., Kuo, C. P., and Garba, J. A., "Direct Structural Parameter Identification by Modal Test Results," *Proceedings of the AIAA/ASME/ASCE/AHS 24th Structures, Structural Dynamics, and Materials Conference*, AIAA, New York, 1983, pp. 44–49.

[10]Collins, J. D., Hart, G. C., Hasselman, T. K., and Kennedy, B., "Statistical Identification of Structures," *AIAA Journal*, Vol. 12, No. 2, 1974, pp. 185–190.

[11]Chen, J. C., and Wada, B. K., "Criteria for Analysis-Test Correlation of Structural Dynamics Systems," *Journal of Applied Mechanics*, Vol. 42, No. 4, 1975, pp. 471–477.

[12]Lallement, G., and Piranda, D., "Localization Methods for Parametric Updating of FE Models," *Proceedings of the 8th UC/SEM International Modal Analysis Conference* (Kissimmee, FL), Society of Experimental Mechanics, Bethel, CT, 1990, pp. 579–585.

[13]Lallement, G., and Zhang, Q., "Inverse Sensitivity Based on the Eigensolutions: Analysis of Some Difficulties Encountered in the Problem of Parametric," *Proceedings of the 13th International Modal Analysis Seminar*, Katholieke Universiteit Leuven, Leuven, Belgium, 1988, pp. 1–16.

[14]Berger, H., Chaquin, J. P., and Ohayon, R., "Finite Element Model Adjustment Using Experimental Modal Data," *Proceedings of the 2nd UC/SEM International Modal Analysis Conference*, Society of Experimental Mechanics, Bethel, CT, 1984, pp. 1–5.

[15]Ojalvo, I. U., and Pilon, D., "Diagnostics for Geometrically Locating Structural Math Errors from Modal Test Data," *Proceedings of the AIAA/ASME/ASCE/AHS 29th Structures, Structural Dynamics, and Materials Conference* (Williamsburg, VA), AIAA, Washington, DC, 1988, pp. 1174–1186.

[16]Mottershead, J. E., "Theory for the Estimation of Structural Vibration Parameters from Incomplete Data," *AIAA Journal*, Vol. 28, No. 3, 1990, pp. 559–561.

[17]Creamer, N. G., and Junkins, J. C., "Identification Method for Lightly Damped Structures," *Journal of Guidance, Control, and Dynamics*, Vol. 11, No. 6, 1988, pp. 571–576.

[18]Berger, H., Ohayon, R., Barthe, L., and Chaquin, J. P., "Parametric Updating of FE Model Using Experimental Simulation: A Dynamic Reaction Approach," *Proceedings of the 8th UC/SEM International Modal Analysis Conference* (Kissimmee, FL), Society of Experimental Mechanics, Bethel, CT, 1990, pp. 180–186.

[19] Bernitsas, M. N., and Tawekal, R., "Structural Model Correlation Using Large Admissible Perturbations in Cognate Space," *AIAA Journal*, Vol. 29, No. 12, 1991, pp. 2222–2232.

[20] Ibrahim, S. R., and Saafan, A. A., "Correlation of Analysis and Test in Modeling of Structures, Assessment and Review," *Proceedings of the 5th UC/SEM International Modal Analysis Conference* (London), Society of Experimental Mechanics, Bethel, CT, 1987, pp. 1651–1660.

[21] Caesar, B., "Update and Identification of Dynamic Mathematical Models," *Proceedings of the 5th UC/SEM International Modal Analysis Conference* (London), Society of Experimental Mechanics, Bethel, CT, 1987, pp. 453–459.

[22] Heylan, W., and Sas, P., "Review of Model Optimization Techniques," *Proceedings of the 5th UC/SEM International Modal Analysis Conference* (London), Society of Experimental Mechanics, Bethel, CT, 1987, pp. 1177–1182.

[23] Crawley, E. F., and O'Donnell, K. J., "A Procedure for Calculating the Damping in Multi Element Space Structures," *Acta Astronautica*, Vol. 15, No. 12, 1987, pp. 987–996.

[24] Park, S., Park, I., and Ma, F., "Decoupling Approximation of Nonclassically Damped Structures," *AIAA Journal*, Vol. 10, No. 9, 1992, pp. 2348–2351.

[25] Ibrahim, S. R., "Dynamical Modeling of Structures from Measured Complex Modes," *AIAA Journal*, Vol. 21, No. 6, 1982, pp. 898–901.

[26] Guyan, R. J., "Reduction of Stiffness and Mass Matrices," *AIAA Journal*, Vol. 3, No. 2, 1965, pp. 380–385.

[27] Hemez, F. M., and Farhat, C., "Bypassing the Numerical Difficulties Associated with the Updating Simultaneously Mass and Stiffness Matrices," *AIAA Journal*, Vol. 33, No. 3, 1995, pp. 539–546.

[28] Hager, W. W., *Applied Numerical Linear Algebra*, Prentice–Hall, Englewood Cliffs, NJ, 1988, pp. 243–248.

A. Berman
Associate Editor